

Land scene classification from remote sensing images using improved artificial bee colony optimization algorithm

Kamenahalli Chandre Gowda Ganashree¹, Ramakrishna Hemavathy¹, Maddur Ramakrishna Anala²

¹Computer Science and Engineering, RV College of Engineering, Bengaluru, Affiliated to Visvesvaraya Technological University, Belagavi, India

²Information Science and Engineering, RV College of Engineering, Bengaluru, Affiliated to Visvesvaraya Technological University, Belagavi, India

Article Info

Article history:

Received Mar 21, 2023

Revised Jul 21, 2023

Accepted Sep 6, 2023

Keywords:

Convolutional neural network
Improved artificial bee colony
optimization

Land scene classification

Multiclass-support vector
machine

Remote sensing

ABSTRACT

The images obtained from remote sensing consist of background complexities and similarities among the objects that act as challenge during the classification of land scenes. Land scenes are utilized in various fields such as agriculture, urbanization, and disaster management, to detect the condition of land surfaces and help to identify the suitability of the land surfaces for planting crops, and building construction. The existing methods help in the classification of land scenes through the images obtained from remote sensing technology, but the background complexities and presence of similar objects act as a barricade against providing better results. To overcome these issues, an improved artificial bee colony optimization algorithm with convolutional neural network (IABC-CNN) model is proposed to achieve better results in classifying the land scenes. The images are collected from aerial image dataset (AID), Northwestern Polytechnical University-Remote Sensing Image Scene 45 (NWPU-RESIS45), and University of California Merced (UCM) datasets. IABC effectively selects the best features from the extracted features using visual geometry group-16 (VGG-16). The selected features from the IABC are provided for the classification process using multiclass-support vector machine (MSVM). Results obtained from the proposed IABC-CNN achieves a better classification accuracy of 96.40% with an error rate 3.6%.

This is an open access article under the [CC BY-SA](https://creativecommons.org/licenses/by-sa/4.0/) license.



Corresponding Author:

Kamenahalli Chandre Gowda Ganashree

Computer Science and Engineering, RV College of Engineering, Bengaluru, Affiliated to Visvesvaraya Technological University

Belagavi, Karnataka, India

Email: ganashree@rvce.edu.in

1. INTRODUCTION

The rapid growth in satellite development has led to an increase in the number of high-resolution remote sensing images. High-resolution remote sensing photographs provide more detailed geographic information than low-resolution ones, which is advantageous for the sectors of agriculture, defense, geology and atmosphere [1], [2]. Remote sensing images further exhibit images with fine resolution, multi-source, expanded range, and quantitative data due to the developing trends in remote sensing satellites, imaging radars, and unmanned aerial vehicle technology. As a result, the classification of vast volumes of remote sensing image data illustrating land areas is a crucial subject of study, researchers have focused on extracting a variety of efficient feature representations throughout the last few decades to enhance the performance of remote sensing image scene categorization [3]–[5]. Remote sensing scene classification can be characterized

as a technique that divides remote sensing scenes into a number of categories in accordance with their contents [6], [7]. Areas with a lot of unstructured data require varying levels of annotation to prevent categorization oversight. However, the majority of remote sensing images that are now in use, lack properly created ontological structures [8], [9], making it impossible to include learned features with high-level semantic interpretations from category labels [10].

High-resolution remote sensing images are frequently used in a range of sizes and include a variety of content, much like multidirectional targets set against a complicated background [11], [12]. Classification of remote sensing scenes is categorized into Handcrafted features, midlevel features, and deep features [13], [14]. The method of feature fusion has emerged as a potential means of enhancing the performance of the deep features extracted from pre-trained convolutional neural networks (CNNs) [15], [16]. A successful CNN with deep learning features can extract various layers of image data for scene semantic classification, and has in-depth domain expertise for identifying and interpreting remote sensing image features [17], [18]. To extract features from images and subsequently create feature representation for scene categorization, deep CNN models are frequently employed as feature learning techniques [19]. An improvised artificial bee colony algorithm is used in this study to choose the pertinent elements for remote sensing scene classification. The related works based on classifying the remote scene are presented as follows:

Xu *et al.* [20] developed an enhanced classification system that utilized a recurrent neural network combined with a random forest (RNN-RF) classifier to classify the images of land scenes obtained from the satellite. The input images were obtained from the UC Merced land (UCM) dataset which consisted of 21 classes of labeled high-resolution images. The RNN-RF classification system provided an effective visual analysis of various features, and also enhanced classification to detect objects. The combination of RNN and RF obtained higher optimization during cross-validation on the UCM dataset and provided multi-scale views with better accuracy during classification. Since UCM is a smaller dataset, the RNN-RF classification system performed well. But for a well-versed dataset, the classification of images using the RNN-RF system remained a challenge.

Li *et al.* [21] developed a multi augmented attention-based convolutional neural network (MAA-CNN) to classify the land scene from high-spatial-resolution remote sensing (HRRS) images. The MAA-CNN captured the region of discrimination from the images of HRRS and performed attention cropping and augmentation. Attention cropping was utilized to improvise the required regions and perform attention maps. The augmentation was utilized to push the attention map channels to obtain various features. Bilinear attention pooling was used to combine the features, and the interclass distance was narrowed using regularized loss function. The MAA-CNN exhibited poor performance in classifying the images for the NWPU-45 dataset.

Xu *et al.* [22] presented a framework based on deep feature aggregation (DFA) using graph convolutional network (GCN) to classify the high spatial resolution (HSR) image obtained from remote sensing. Initially, the feature extraction was performed using the pre-trained VGG-16 to obtain multiple layers of features. GCN extracted the feature maps of each layer and provided scenes of HSR images by generating a graph for undirected adjacency. The multiple features produced by VGG-16 were combined using the weighted concatenation method. At last, the images were predicted using a linear classifier. However, the DFA-GCN faced consequences in classifying similar ground objects like man-made structures and roads.

Shen *et al.* [23] presented a dual-model architecture along grouping attention fusion strategy to improvise the efficiency in land scene classification. The dual model consisted of two CNNs to extract the features, and a grouping attention fusion strategy was utilized to combine the CNN features in a multi-scale way. A loss function was generated for diversities in small intra classes and large inter-class distances that produced an enhanced classification performance. The dual model architecture showed better performance than the single CNN model by providing enhanced feature selection. However, misclassification occurred in classifying similar objects.

Guo *et al.* [24] introduced a saliency dual attention residual network (SDAResNet) to mine the cross-channels and spatial information, for classifying land scenes in remote sensing images. The SDAResNet consists of two types of attention: spatial attention and channel attention, where the spatial attention was embedded in a low-level feature to highlight and quash information on the background. The channel attention was utilized for combining the high feature levels to mine information from meaningful saliencies. The land scene classification using SDAResNet utilized an attention mechanism and offered a better classification accuracy. However, the challenge was faced in classifying the natural images such as trees, and mountains, since they appeared similar in visual aspect.

The major contributions of this research are listed as follows:

- a. The artificial bee colony (ABC) optimization algorithm is in remote sensing land scene classification, but it produces poor classification accuracy using probability selection. To overcome this issue, the improved

- artificial bee colony (IABC) optimization algorithm is proposed, which performs based on neighborhood selection and helps the classifier to provide better classification results.
- b. Feature extraction is performed with the help of VGG-16, where the image data is converted into array data which helps to extend the dimensions of the array with various sizes.
 - c. This research employs MSVM to create an optimal hyperplane and classifies it into a linear pattern. MSVM verifies the input pattern and performs classification, providing better classification results in lower dimensions.

The remaining paper is organized as follows: section 2 presents a detailed explanation of the IABC algorithm. The results and discussion are provided in section 3. Finally, section 4 represents the overall conclusion of this paper.

2. IABC OPTIMIZATION ALGORITHM FOR FEATURE SELECTION

The classification of land scenes from the remote sensing images is a challenging process in remote sensing interpretation. This research proposed an IABC optimization algorithm that is employed in feature selection. The features selected using the proposed IABC make classification process easier, by providing better accuracy and removing unnecessary partitions from the image. A detailed description of the overall process involved in land scene classification is discussed in the following sections. The overall process involved in the classification process is diagrammatically represented in Figure 1.

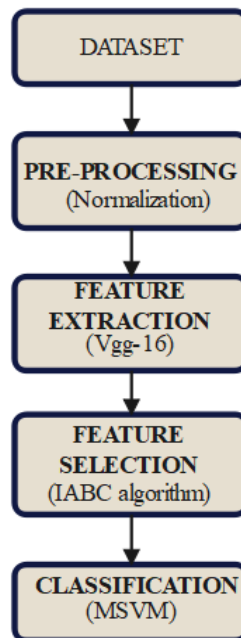


Figure 1. Process involved in the classification of remote sensing land scenes

2.1. Dataset

This research made use of three publicly available datasets based on land scene classification using remote sensing technology to evaluate the efficiency of the proposed method. The three datasets include aerial image dataset (AID), Northwestern Polytechnical University-Remote Sensing Image Scene 45 (NWPU-RESIS45), and University of California Merced (UCM) dataset. The descriptions of the aforementioned datasets are provided in the following sub-sections:

2.1.1. AID

The AID [25] is collected from Google Earth by Wuhan University which consists of a large-scale land-use dataset for HRRS images with 30 land scenes. The 30 land scenes include airports, parking, stadium, beach, schools, desert, farmland, meadow, bridge, and port. The AID dataset includes 10,000 images with a pixel size of 600×600 for every individual image and these images are labeled by remote sensing image experts.

2.1.2. NWPU-RESIS45

The NWPU-45 [26] is one of the challenging databases for classifying HRRS images. The database contains 45 category HRRS images with a pixel size of 256×256 in the color space of red, green, and blue (RGB) and each category in NWPU-45 consists of 700 images. The NWPU-45 dataset contains about 31,500 images in total. The 45 categories contain commercial plots, forests, mountains, harbors, and these categories consist of abundant images. The images in various categories seem to be similar, so it is quite challenging to attain superior performance with these images.

2.1.3. UCM dataset

The UCM dataset [27] is utilized in classifying the various surfaces of land obtained from high-resolution remote sensing images. The UCM dataset is collected from USGS University of California, Merced which is categorized into 21 classes with a total of 2,100 images. Each image present in the UCM dataset has a pixel size of 256×256 .

2.2. Pre-processing

After collecting the data from the datasets, pre-processing is necessary to be performed. In this research, the collected data is initially processed by radiometric and geometric modifications followed by clipping of images. The useless portions present in the images are removed, while the noises and discrepancies present in the image are detached using digital filters.

2.2.1. Normalization

Normalization is an essential process that aids to ease the extraction of features and classification of remote-sensing land scenes. Normalization is defined as processing the images for varying values of pixel intensities. In this research, the image data is scaled using min-max normalization to improvise the learning speed. The normalization function takes image data x and produces a normalized image. The intensity of the image may be in the range of 0 to 255 and sometimes in negative values, so min-max normalization is applied to the input image data and is transformed in the range of 0 to 1. The min-max normalization is computed using (1).

$$N = \frac{x - V_{min}}{V_{max} - V_{min}} \quad (1)$$

where the maximum and minimum values of the pixels are represented as V_{max} and V_{min} respectively. The output from normalization is provided as input for the process of feature extraction.

2.3. Feature extraction

The normalized output image is provided as the input for the feature extraction process. In this research, the visual geometry group-16 (VGG-16), which is a convolutional neural network (CNN) model, is deployed to extract the deep features from the image. Since VGG-16 provides better accuracy value for the ImageNet dataset (a vast dataset with around fifteen million images), it is utilized in this research. The VGG-16 has 13 convolutional layers where the size of the filter is 3×3 and the pooling layer has the size of 2×2 . Moreover, two fully connected layers along with a soft max function are present in the architecture of VGG-16. In VGG-16, the image data is converted into array data which helps to extend the dimensions of the array with various sizes. Generally, the architecture of the VGG-16 model is deep and helps to adjust the values of pixels, which efficiently aids in extracting the features from the image data. The architectural diagram of the VGG-16 model is represented in Figure 2.

2.4. Feature selection using IABC optimization algorithm ABC optimization

There are various types of optimization algorithms introduced from inspiration by nature. Likewise, the ABC algorithm is inspired by the intelligent behavior of bees. Generally, bees keep on trying to search for a better source of food with more nectar. The bees present in the swarm are categorized into three categories namely, employer bee, onlooker bee, and scout bee. In the process of iteration, the bees perform various operations to get a good source of nectar. In the initial stage, the swarm has S solutions, and the i^{th} iteration of solution X_i to find the food in the swarm is represented in (2).

$$X_i = x_{i,1}, x_{i,2}, \dots, x_{i,D} \quad (2)$$

where S is known as swarm size, x_i is abandoned solution, and the dimension size is denoted as D . The complete operation process involved in the food search of ABC is mentioned below.

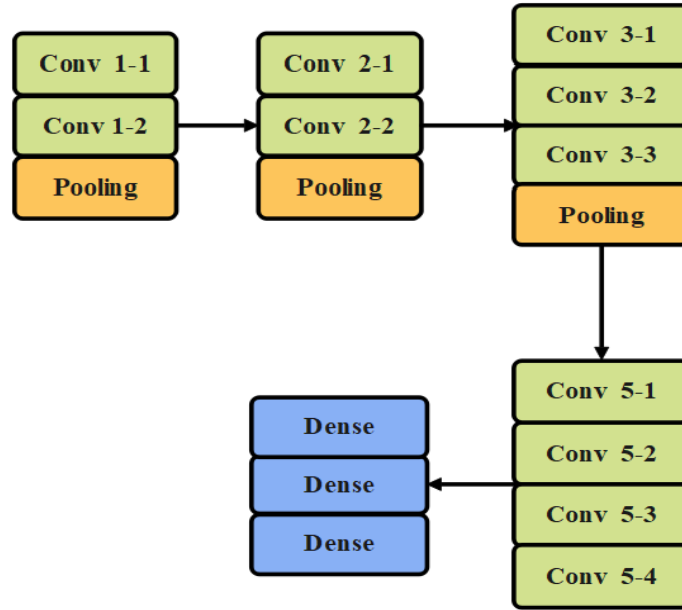


Figure 2. Architecture of VGG-16

2.4.1. Search phase of employer bee

In this stage, the employer bee searches for an optimal solution and operates to identify a good source of food.

$$V_{i,jr}^* = X_{i,jr} + \phi_{i,jr} \cdot (X_{i,jr} - X_{k,jr}) \tag{3}$$

where the variable $V_{i,jr}^*$ is used to provide candidate food position, the value taken from the whole swarm is denoted as X_k and the random integer is denoted as jr which lies in the range $[1, D]$. The weighted function created among the range -1 and 1 is denoted as $\phi_{i,jr}$. When the search for employer bee is completed as per (3), the new solution V_i is created which is represented in (4).

$$V_{i,j} = \begin{cases} V_{i,jr}^* & \text{if } j = jr \\ X_{i,j} & \text{otherwise} \end{cases} \tag{4}$$

where the value of $j = 1, 2, \dots, D$. To obtain a better solution, a methodology based on greedy selection is used which is mentioned in (5).

$$X_i = \begin{cases} V_i, & \text{if } V_i \text{ outperforms } X_i \\ X_i, & \text{otherwise} \end{cases} \tag{5}$$

2.4.2. Search phase of onlooker bee

In this stage, the neighborhood search for all solutions is completed using the employer bees. After this, the onlooker bees obtain the information from the employer bees. Some of the best solutions are chosen to proceed with the search at this phase. The better solution is described by selecting the probability p_i for every individual solution. The probability p_i is evaluated using the formula mentioned in (6).

$$p_i = \frac{fit(X_i)}{\sum_{i=1}^S fit(X_i)} \tag{6}$$

where the fitness value of X_i is denoted as $fit(X_i)$ and it is computed using (7).

$$fit(X_i) = \begin{cases} \frac{1}{1+|f(X_i)|}, & \text{if } f(X_i) \geq 0 \\ 1 + |f(X_i)|, & \text{if } f(X_i) < 0 \end{cases} \tag{7}$$

where the value of the objective function X_i is represented as $f(X_i)$. For every onlooker bee in the swarm, the better solution X_i is chosen based on p_i value. A new offspring is created using the (3) and (4), and a better solution is obtained among X_i and V_i .

2.4.3. Search phase of the scout bee

Based on (5), a new solution is created with the solution from their parents. The search in the neighborhood becomes successful when V_i is better than X_i , and the search in neighborhood also denotes when V_i is worse than X_i . The search of the neighborhood is monitored using a failure counter $trial_i$. When the search becomes successful, the $trial_i$ is set as 0 and when the search becomes a failure, $trial_i$ is added as 1. The updated $trial_i$ is mentioned in (8).

$$trial_i = \begin{cases} 0, & \text{if } V_i \text{ is better than } X_i \\ trial_i + 1, & \text{otherwise} \end{cases} \quad (8)$$

When the value of $trial_i$ is greater than the limit, the respective solution X_i is prohibited. The prohibited X_i is replaced using (9).

$$x_{i,j} = low + rand(0,1) \cdot (up_j - low_j) \quad (9)$$

where the value of $j = 1, 2, \dots, D$ and the randomly created value in the range $[0, 1]$ is denoted as $rand(0, 1)$. The marginal limitation for the upper limit and the lower limit is denoted as up_j and low_j respectively.

2.5. Improvised artificial bee colony optimization

The ABC optimization algorithm is improvised using the neighborhood selection method. The conversion of ordinary ABC optimization to an improvised ABC includes changes such as the developing of neighborhood selection, which replaces probability selection. The altered search approaches are created and finally the search phase of the scout bee is improvised using a radius of the neighborhood.

2.5.1. Selection of neighborhood

The development of selection of neighborhoods is made, which is applied instead of probability selection. The solutions present in the colonies create a ring formation where the methodology of k-neighborhood is utilized, and k is the parameter of the neighboring radius. The k-neighborhood methodology consists of solutions of $2k + 1$, when the neighboring radius fulfills the condition that $1 \leq k \leq \frac{S-1}{2}$. In every individual solution in the swarm X_i , the worthy solution X_{ib} is selected in the k-neighborhood methodology. In the proposed methodology, the selection probability does not need to be chosen for every individual solution.

2.5.2. Altered search approach

The k-neighborhood methodology is used in an altered search approach for employer bees. In the previous section, X_i is replaced by a worthy solution X_{ib} . So, the employer bees need not search for the neighborhood for every solution of X_i , and so the search is performed for the solution X_{ib} only. In (10) provides an altered search approach as (10).

$$V_{i,jr}^* = X_{ib,jr} + \phi_{i,jr} \cdot (X_{ib,jr} - X_{k,jr}) + \phi_{i,jr} \cdot (X_{best,jr} - X_{ib,jr}) \quad (10)$$

where the best solution obtained from k-neighborhood is denoted as X_{ib} . According to (4) and (10), a new solution V_i is obtained. For i^{th} onlooker bee, k neighborhood selects the X_{ib} which is represented in (11).

$$V_{ib,jr}^* = X_{ib,jr} + \phi_{i,jr} \cdot (X_{ib,jr} - X_{k,jr}) + \phi_{i,jr} \quad (11)$$

$$V_{ib,j} = \begin{cases} V_{ib,jr}^*, & \text{if } f(V_{ib}) < f(X_{ib}) \\ X_{ib,j}, & \text{otherwise} \end{cases} \quad (12)$$

where $j = 1, 2, \dots, D$. According to the values from V_{ib} and X_{ib} , the better solution is selected based on (13).

$$X_i = \begin{cases} V_{ib}, & \text{if } f(V_{ib}) < f(X_{ib}) \\ X_{ib}, & \text{otherwise} \end{cases} \quad (13)$$

2.5.3. Altered search phase using scout bee

In the solution X_i , each status is controlled by $trial_i$. When the $trial_i \geq limit$, the solution X_i is neglected. After this a new X_i is created as a substitute for a neglected solution. When the search space in the swarm of scout bees decreases, a random solution is included to improvise the search region. Neglecting the solution X_i , three solutions U_1, U_2 , and U_3 are produced, and the best solution among the three is chosen to replace the neglected X_i . The value of U_1 is created randomly, same as in the ABC algorithm which is previously described in (9). U_2 is created from k -neighborhood and the best solution X_{ib} is selected. This can be represented mathematically as (14).

$$U_{2,j} = X_{ib,j} + rand(0,1) \cdot (X_{r1,j} - X_{r2,j}) \quad (14)$$

where $j = 1, 2, \dots, D$ and the two randomly chosen solutions from the scout bee swarm are denoted as X_{r1} and X_{r2} .

In U_3 , X_{ib} is chosen as the best neighbor from the neglected solution of k -neighborhood. The generation of U_3 takes place according to (15).

$$U_{3,j} = X_j^{min} + X_j^{max} - X_{ib,j} \quad (15)$$

The values of X_j^{min} and X_j^{max} are denoted as $\min\{X_{i,j}\}$ and $\max\{X_{i,j}\}$ respectively. The value of i lies between the range of $[1-S]$, and j lies between the range of $[1-D]$. Where the boundaries of the scout bee are represented as X_j^{min} and X_j^{max} . When all the solutions of U_1, U_2 and U_3 are created, the best of three solutions is chosen to replace the neglected X_i . Thus the best feature is selected using the proposed IABC optimization algorithm. The fitness evaluation in IABC is performed based on the neighborhood selection method and is evaluated using (16).

$$fit(X_i) = \begin{cases} \frac{1}{1+f(X_i)}, & \text{if } f(X_i) \geq 0 \\ 1 + |f(X_i)|, & \text{if } f(X_i) < 0 \end{cases} \quad (16)$$

where the objective value is denoted as $f(X_i)$.

2.6. Classification

The high-resolution remote sensing images obtained from the feature selection process undergo the process of classification where the various land scenes are classified. The classification of land scenes is performed using multiclass-support vector machine (MSVM). The features selected using IABC are given as input to obtain an accurate classification of remote sensing images that are acquired from the various datasets discussed previously. The MSVM is created by combining multiple-binary SVM in the classification process. The MSVM is used to create an optimal hyperplane and then classifies it into a linear pattern. MSVM verifies the input pattern and performs classification, which provides better classification results in lower dimensions.

3. RESULTS AND ANALYSIS

This section provides the results and analysis of this research. The result portion is classified into performance analysis and comparative analysis, represented in the following sections. In performance analysis, the efficiency of the classifier is evaluated and the efficacy of the optimization algorithm inclusive of the proposed approach is evaluated. In comparative analysis, the performance of the proposed approach is evaluated with the existing approaches.

3.1. Performance analysis

The performance of the MSVM classifier with feature selection is compared with the existing classifiers namely, k-nearest neighbor (KNN), naïve Bayes (NB), support vector machine (SVM) and multiclass support vector machine (MSVM). The performance analysis of the classifier with feature selection is represented in Table 1. In Table 1, it is shown that feature selection using IABC with the MSVM classifier performs better than the existing classifiers that are, KNN, NB, SVM, and MSVM. MSVM classifier combines multiple binaries during the classification process, and performs classification in a linear pattern, thus acting as a reason to provide better classification in lower dimensions. The MSVM attained an accuracy of 96.96%, which is comparatively higher than that of KNN (94.23%), NB (95.28%) and SVM (95.55%). The performance of classifiers with feature selection is graphically represented in Figure 3.

Table 1. Performance analysis of various classifiers with feature selection

Classifier	Accuracy (%)	Sensitivity (%)	Specificity (%)	F1-score (%)	Error rate (%)
KNN	94.23	92.79	96.91	94.93	5.77
NB	95.28	91.96	93.79	92.82	4.72
SVM	95.55	92.80	93.96	95.24	4.45
MSVM	96.40	97.00	94.91	95.46	3.6

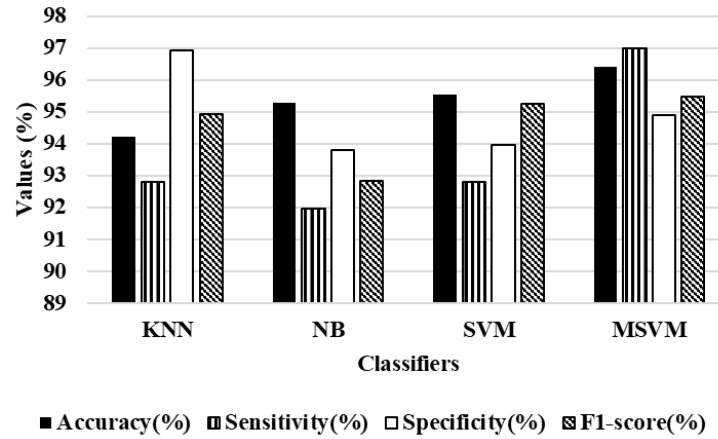


Figure 3. Graphical representation of classifiers with feature selection

Table 2 shows the classification performance of the MSVM classifier without the feature selection process. The performance of MSVM is reduced without the feature selection process which helps in providing a selected feature and eases the classification process. Although, MSVM classifier performs well when compared to the existing classifiers such as KNN, NB, and SVM. The analyses from Tables 1 and 2 exhibit the significance of the feature selection process. Therefore, feature selection is important in providing better classification accuracy. The performance of classifiers without feature selection is graphically represented in Figure 4.

Table 2. Performance analysis of various classifiers without feature selection

Classifier	Accuracy (%)	Sensitivity (%)	Specificity (%)	F1-score (%)	Error rate (%)
KNN	91.23	91.86	91.32	90.56	8.77
NB	90.28	89.63	91.79	89.27	9.72
SVM	92.55	90.18	93.96	92.46	7.45
MSVM	93.45	95.81	94.56	93.32	6.45

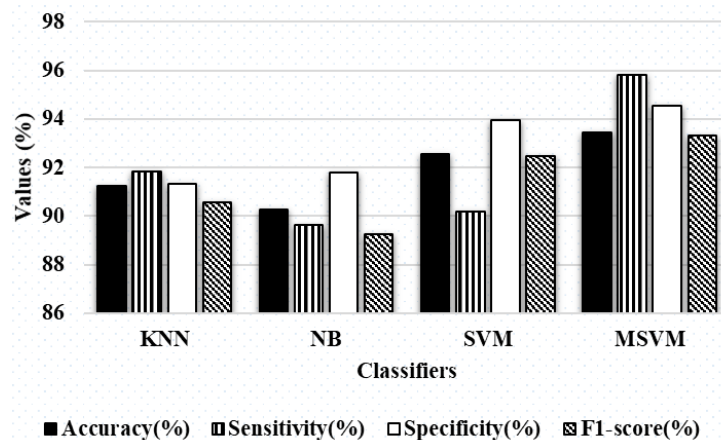


Figure 4. Graphical representation of classifiers without feature selection

3.2. Performance of optimization algorithms

In this research, the feature selection process is performed using IABC optimization algorithm. IABC algorithm is an advanced optimization technique of ABC where neighborhood selection is involved, instead of probability selection. Here, the performance of IABC optimization with the existing optimization algorithms such as particle swarm optimization (PSO), ant colony optimization (ACO), fruit fly optimization algorithm (FOA), ABC optimization, and IABC optimization algorithms are evaluated based on parameters like accuracy, sensitivity, specificity, F1 score and error rate. Table 3 provides the performance of various optimization algorithms.

From Table 3, it is seen that the performance of IABC optimization algorithm is better when compared with other optimization algorithms. Due to improved search strategies and selection using the neighborhood method, the IABC achieved better results. It achieved a better classification accuracy of 96.40% and a less error rate of 3.6%. The performance of optimization algorithms is graphically represented in Figure 5.

Table 3. Performance of optimization algorithm

Algorithms	Accuracy (%)	Sensitivity (%)	Specificity (%)	F1-score (%)	Error rate (%)
PSO	87.66	90.27	89.93	90.49	12.34
ACO	92.35	91.70	90.99	91.34	7.65
FOA	94.78	93.36	92.16	93.73	5.22
ABC	94.96	94.25	93.25	94.91	5.04
IABC	96.40	97.00	94.91	95.46	3.6

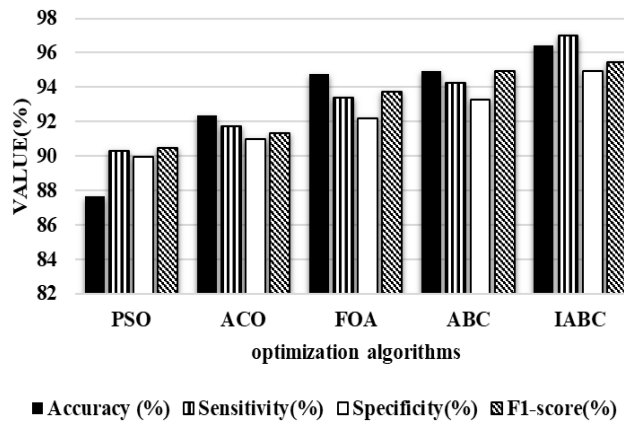


Figure 5. Graphical representations for the performance of the optimization algorithm

3.3. Comparative analysis

The comparative analysis of the proposed IABC-CNN with the existing methodologies namely, multi-augmented attention-based convolutional neural network (MAA-CNN) [20] and deep feature aggregation framework driven by graph convolutional network (DFAGCN) [22] is discussed in this section with regard to classifying land scenes in remote sensing data. The comparative table of the proposed IABC-CNN with existing MAA-CNN [20] and DFAGCN [22] is represented in Table 4.

From the above comparative Table 4, it is shown that the proposed IABC-CNN exhibits better performance when compared with existing methodologies, MAA-CNN [20] and DFAGCN [22]. The CNN model (VGG-16) is used for feature extraction and IABC algorithm is used for selecting the optimal features. The IABC is utilized in selecting the features which are extracted from the CNN model. The extracted features reduce the redundancy and increase the learning speed. These extracted features are selected using the proposed IABC algorithm, which aids in better classification of land scenes in HRRS images. The IABC-CNN provides better classification accuracy of 96.40%, which is comparatively higher than the MAA-CNN (91.67%) and DFAGCN (88.50%).

Table 4. Comparative table

Methods	Accuracy (%)	Sensitivity (%)	Specificity (%)	F1-score (%)
MAA-CNN [15]	91.67	71.67	95	78.33
DFAGCN [17]	88.50	83.50	86	83
IABC-CNN	96.40	97.00	94.91	95.46

4. CONCLUSION

Remote-sensed photographs play a significant role in monitoring environmental conditions, disaster mitigation and other remote sensing applications. Due to complex backgrounds, poor imaging conditions and similarities, it is difficult to classify the remote sensing images on various land surfaces. In this research, the input images are obtained from three familiar datasets: AID, NWPU-RESIS45, and UCM dataset. The input images are pre-processed using the normalization technique, where they are adjusted for the intensities of the pixels. The preprocessed images undergo feature extraction using VGG-16 model where the values of pixels are efficiently extracted from the image data. Then feature selection is performed using the proposed IABC algorithm, which selects the significant features and finally, the remote sensing land scene images are classified using the MSVM classifier. The experimental results show that the proposed IABC-CNN model delivered better performance than the existing MAA-CNN and DFAGCN by providing better classification accuracy of 96.40% while MAA-CNN and DFAGCN achieved 91.67% and 88.50%, respectively. In the future, the research work can be extended by using deep learning models to improve classification accuracy during categorizing land surfaces.




REFERENCES

- [1] K. Xu, H. Huang, P. Deng, and G. Shi, "Two-stream feature aggregation deep neural network for scene classification of remote sensing images," *Information Sciences*, vol. 539, pp. 250–268, Oct. 2020, doi: 10.1016/j.ins.2020.06.011.
- [2] M. Li, L. Lei, Y. Tang, Y. Sun, and G. Kuang, "An attention-guided multilayer feature aggregation network for remote sensing image scene classification," *Remote Sensing*, vol. 13, no. 16, Aug. 2021, doi: 10.3390/rs13163113.
- [3] X. Zhao, J. Zhang, J. Tian, L. Zhuo, and J. Zhang, "Residual dense network based on channel-spatial attention for the scene classification of a high-resolution remote sensing image," *Remote Sensing*, vol. 12, no. 11, Jun. 2020, doi: 10.3390/rs12111887.
- [4] S.-C. Hung, H.-C. Wu, and M.-H. Tseng, "Remote sensing scene classification and explanation using RSSNet and LIME," *Applied Sciences*, vol. 10, no. 18, Sep. 2020, doi: 10.3390/app10186151.
- [5] Q. Wang, W. Huang, Z. Xiong, and X. Li, "Looking closer at the scene: multiscale representation learning for remote sensing image scene classification," *IEEE Transactions on Neural Networks and Learning Systems*, vol. 33, no. 4, pp. 1414–1428, Apr. 2022, doi: 10.1109/TNNLS.2020.3042276.
- [6] H. Alhichri, A. S. Alswayed, Y. Bazi, N. Ammour, and N. A. Alajlan, "Classification of remote sensing images using EfficientNet-B3 CNN model with attention," *IEEE Access*, vol. 9, pp. 14078–14094, 2021, doi: 10.1109/ACCESS.2021.3051085.
- [7] J. Shen, T. Yu, H. Yang, R. Wang, and Q. Wang, "An attention cascade global-local network for remote sensing scene classification," *Remote Sensing*, vol. 14, no. 9, Apr. 2022, doi: 10.3390/rs14092042.
- [8] C. Peng, Y. Li, L. Jiao, and R. Shang, "Efficient convolutional neural architecture search for remote sensing image scene classification," *IEEE Transactions on Geoscience and Remote Sensing*, vol. 59, no. 7, pp. 6092–6105, Jul. 2021, doi: 10.1109/TGRS.2020.3020424.
- [9] X. Gu, C. Zhang, Q. Shen, J. Han, P. P. Angelov, and P. M. Atkinson, "A self-training hierarchical prototype-based ensemble framework for remote sensing scene classification," *Information Fusion*, vol. 80, pp. 179–204, Apr. 2022, doi: 10.1016/j.inffus.2021.11.014.
- [10] S. Wang, Y. Guan, and L. Shao, "Multi-granularity canonical appearance pooling for remote sensing scene classification," *IEEE Transactions on Image Processing*, vol. 29, pp. 5396–5407, 2020, doi: 10.1109/TIP.2020.2983560.
- [11] Y. Y. Ghadi, A. A. Rafique, T. al Shloul, S. A. Alsuhibany, A. Jalal, and J. Park, "Robust object categorization and scene classification over remote sensing images via features fusion and fully convolutional network," *Remote Sensing*, vol. 14, no. 7, Mar. 2022, doi: 10.3390/rs14071550.
- [12] S.-B. Chen, Q.-S. Wei, W.-Z. Wang, J. Tang, B. Luo, and Z.-Y. Wang, "Remote sensing scene classification via multi-branch local attention network," *IEEE Transactions on Image Processing*, vol. 31, pp. 99–109, 2022, doi: 10.1109/TIP.2021.3127851.
- [13] O. Sen and H. Y. Keles, "A hierarchical approach to remote sensing scene classification," *PFG-Journal of Photogrammetry, Remote Sensing and Geoinformation Science*, vol. 90, no. 2, pp. 161–175, Apr. 2022, doi: 10.1007/s41064-022-00193-0.
- [14] W. Tong, W. Chen, W. Han, X. Li, and L. Wang, "Channel-attention-based densenet network for remote sensing image scene classification," *IEEE Journal of Selected Topics in Applied Earth Observations and Remote Sensing*, vol. 13, pp. 4121–4132, 2020, doi: 10.1109/JSTARS.2020.3009352.
- [15] D. Wang, C. Zhang, and M. Han, "MLFC-net: A multi-level feature combination attention model for remote sensing scene classification," *Computers and Geosciences*, vol. 160, Mar. 2022, doi: 10.1016/j.cageo.2022.105042.
- [16] B. Yuan, L. Han, X. Gu, and H. Yan, "Multi-deep features fusion for high-resolution remote sensing image scene classification," *Neural Computing and Applications*, vol. 33, no. 6, pp. 2047–2063, Mar. 2021, doi: 10.1007/s00521-020-05071-7.
- [17] X. Sun, Q. Zhu, and Q. Qin, "A multi-level convolution pyramid semantic fusion framework for high-resolution remote sensing image scene classification and annotation," *IEEE Access*, vol. 9, pp. 18195–18208, 2021, doi: 10.1109/ACCESS.2021.3052977.
- [18] A. Ma, Y. Wan, Y. Zhong, J. Wang, and L. Zhang, "SceneNet: Remote sensing scene classification deep learning network using multi-objective neural evolution architecture search," *ISPRS Journal of Photogrammetry and Remote Sensing*, vol. 172, pp. 171–188, Feb. 2021, doi: 10.1016/j.isprsjprs.2020.11.025.
- [19] E. Li, A. Samat, P. Du, W. Liu, and J. Hu, "Improved bilinear CNN model for remote sensing scene classification," *IEEE Geoscience and Remote Sensing Letters*, vol. 19, pp. 1–5, 2022, doi: 10.1109/LGRS.2020.3040153.
- [20] X. Xu, Y. Chen, J. Zhang, Y. Chen, P. Anandhan, and A. Manickam, "A novel approach for scene classification from remote sensing images using deep learning methods," *European Journal of Remote Sensing*, vol. 54, pp. 383–395, Mar. 2021, doi: 10.1080/22797254.2020.1790995.
- [21] F. Li, R. Feng, W. Han, and L. Wang, "An augmentation attention mechanism for high-spatial-resolution remote sensing image scene classification," *IEEE Journal of Selected Topics in Applied Earth Observations and Remote Sensing*, vol. 13, pp. 3862–3878, 2020, doi: 10.1109/JSTARS.2020.3006241.
- [22] K. Xu, H. Huang, P. Deng, and Y. Li, "Deep feature aggregation framework driven by graph convolutional network for scene classification in remote sensing," *IEEE Transactions on Neural Networks and Learning Systems*, vol. 33, no. 10, pp. 5751–5765, Oct. 2022, doi: 10.1109/TNNLS.2021.3071369.




- [23] J. Shen, T. Zhang, Y. Wang, R. Wang, Q. Wang, and M. Qi, "A dual-model architecture with grouping-attention-fusion for remote sensing scene classification," *Remote Sensing*, vol. 13, no. 3, Jan. 2021, doi: 10.3390/rs13030433.
- [24] D. Guo, Y. Xia, and X. Luo, "Scene classification of remote sensing images based on saliency dual attention residual network," *IEEE Access*, vol. 8, pp. 6344–6357, 2020, doi: 10.1109/ACCESS.2019.2963769.
- [25] G.-S. Xia *et al.*, "AID: A benchmark data set for performance evaluation of aerial scene classification," *IEEE Transactions on Geoscience and Remote Sensing*, vol. 55, no. 7, pp. 3965–3981, Jul. 2017, doi: 10.1109/TGRS.2017.2685945.
- [26] G. Cheng, J. Han, and X. Lu, "Remote sensing image scene classification: benchmark and state of the art," *Proceedings of the IEEE*, vol. 105, no. 10, pp. 1865–1883, Oct. 2017, doi: 10.1109/JPROC.2017.2675998.
- [27] Y. Yang and S. Newsam, "Bag-of-visual-words and spatial extensions for land-use classification," in *Proceedings of the 18th SIGSPATIAL International Conference on Advances in Geographic Information Systems*, Nov. 2010, pp. 270–279, doi: 10.1145/1869790.1869829.

BIOGRAPHIES OF AUTHORS






Kamenahalli Chandre Gowda Ganashree    working as assistant professor in R.V. College of Engineering in Department of Computer Science and Engineering. I am currently working for my research in traffic monitoring using aerial images. She can be contacted at email: ganashree@rvce.edu.in.



Ramakrishna Hemavathy    working as associate professor in the Department of CSE at RVCE Bengaluru. She has 20+ years of rich experience in teaching. Her area of interests is image processing, computer vision, machine learning and artificial neural networks. She has published more than 40+ papers in international, national journals, conferences. She can be contacted at email: hemavathyr@rvce.edu.in.



Maddur Ramakrishna Anala    is working as professor at R.V. College of Engineering. She has over 20+ years of experience in Teaching and Research. Her area of research includes deep learning, computer architecture, high performance computing, distributed systems and parallel programming. She has guided more than 70 UG and PG projects. She has published over 70+ papers in national and international journals and conferences. She can be contacted at email: analamr@rvce.edu.in.